Vibration Serviceability of Building Floors: Performance Evaluation of Contemporary Design Guidelines

Zandy O Muhammad[1] and Paul Reynolds[2]

[1]PhD Student, College of Engineering, Mathematics and Physical Sciences, Vibration Engineering Section, University of Exeter, UK. Email: zm247@exeter.ac.uk

[2]Professor of Structural Dynamics and Control, College of Engineering, Mathematics and Physical Sciences, Vibration Engineering Section, University of Exeter, UK. Email: p.reynolds@exeter.ac.uk

ABSTRACT

The drive towards innovative design of structural systems assisted by more efficient materials has resulted in ever more slender spans and lighter weight constructions. This has also been accompanied by the growing trend of open-plan floor developments with fewer internal partitions. As a consequence, concerns are increasingly expressed over excessive human-induced vibrations under normal in-service conditions. These floors might be considered to fail to meet the vibration serviceability criterion, even though in some cases they may satisfy the requirements of existing vibration design guidelines and tolerance limits. Thus, this paper outlines a thorough back analysis of three tested full-scale floors with respective finite element modeling to evaluate the reliability of contemporary guidelines. It is demonstrated that current forms of design guidance may require significant improvements in the key aspects of walking load models, response prediction and threshold tolerance in order to more reliably predict the actual vibration response and corresponding vibration assessment.

INTRODUCTION

Excessive vibrations induced by pedestrians are frequently surfacing in contemporary civil engineering structures, such as footbridges (Zivanović et al. 2007) and floors (Nguyen 2013; Hudson

and Reynolds 2014). These are often a result of advancements in the construction sector resulting in innovative structural designs, allowing design engineers to roll out ever more slender, lightweight and more flexible systems. Floors, as an integral element of any building, not only characterized by larger spans, lighter weight and relatively less damping due to the growing drive towards open-plan layouts with fewer partition walls, but also possess particular dynamic features, such as closely-spaced mode shapes (Pavic et al. 2008), higher uncertainties in modal parameters (Reynolds and Pavic 2003) and subjective judgements on vibration magnitude by different occupants (Setareh 2009). The potential for annoying vibrations remains high under human-induced loadings. As a consequence, vibration serviceability design is a major challenge in modern floor design whereby the prediction of vibration responses under human-induced footfall remains a difficult task.

Several design guidelines, as listed below, are available at the design stage to predict the vibration responses and provide methodologies for assessment of vibration serviceability of floors under pedestrian-induced vibrations.

- American Institute of Steel Construction Design Guide 11 (AISC DG11) (Murray et al. 2016)
- Design Guide for Vibrations of Reinforced Concrete Floor Systems, Concrete Reinforcing Steel Institute (CRSI) (Fanella and Mota 2014)
- Steel Construction Institute publication 354 (SCI P354) (Smith et al. 2009)
- European guideline, Human Induced Vibration of Steel Structures 2007 (HiVoSS) (RFCS 2007a; RFCS 2007b)
- Concrete Centre Industry Publication 016 (CCIP-016) (Willford and Young 2006)
- Concrete Society Technical Report 43 Appendix G (CSTR43 App G) (Pavic and Willford 2005)

The application of current guidelines is generally for a single pedestrian at the design stage, where a deterministic walking load model is utilized to represent actual walking. Even though numerous studies (Brownjohn et al. 2004; Zivanović et al. 2007) have shown that such an approach is

unable to reliably describe walking and its innate variabilities, nevertheless contemporary guidance documents display significant dependence on that force model. Thus, the provided design methods often result in inaccurate vibration responses (Hassan and Girhammar 2013; Brownjohn et al. 2016). The main shortcomings can be summarized as follows (Feldmann et al. 2009):

- Lack of a pedestrian load model with sufficient reliability as the excitation source; thus a probabilistic approach is needed (Zivanović 2006; Nguyen 2013).
- Incorrect characterization of floor properties in terms of their modal parameters (modal mass, natural frequency and damping ratio), in particular modal masses (Middleton 2009).
- Uncorroborated simplifying assumptions, such as considering partition walls as damping elements and ignoring their mass and stiffness contribution.
- Imprecise assessment of floor response according to relevant vibration descriptors (Setareh 2009) and tolerance thresholds. In some cases, different tolerance limits are given in different guidelines for the same vibration metric (e.g. Response factor (R factor)) (Muhammad et al. 2017).

The main objective of this paper is to appraise a number of widely used vibration guidelines (AISC DG11, SCI P354, HiVoSS, CCIP-016 and CSTR43 App G) and evaluate the methodologies applied in the analysis and design of floors whose vibration responses are of concern. The procedures given in each guideline are based on certain assumptions and simplifications, but a systematic assessment of the actual efficacy is required to reflect current design practice with respect to the full-scale floors under normal in-service conditions. The efficacy and assessment of the design guidance are carried out through three tested full-scale floors involving their respective finite element (FE) modeling. Both simplified and FE approaches recommended by the guidance documents are used to predict the vibration response. To facilitate reliable evaluations, the predicted response metrics are compared with those from measurements.

CONTEMPORARY GUIDELINES AND CODES OF PRACTICE

The following section gives a brief overview of vibration design methodologies of the current

guidelines. The design methods will be describing methodologies pertinent to low-frequency floors (LFF); those that exhibit primarily resonant response. For high-frequency floors (HFF) the reader is referred to (Middleton 2009; Liu and Davis 2015).

AISC DG11

AISC DG11 (Murray et al. 2016) deals with the vibration serviceability of steel framed structures. This guidance's response methodology used in this paper is summarized in Fig.1. The vibration response is computed based on the frequency threshold; if the fundamental frequency is below 9 Hz, the response under walking is predominantly resonant and can be described by a sinusoidal peak acceleration (equivalent R factor=sinusoidal peak acceleration x 0.707 divided by the reference value of 0.005 m/s^2 (ISO10137 2007)). In the case of floors whose fundamental frequency is above this limit, a transient response to a single impulse footstep is deemed more appropriate.

Frequency Response Functions (FRFs) are used to determine the dominant mode shapes and frequencies. The FRF magnitudes are computed via harmonic or steady-state analysis for a unit load at the walking load location (i.e a stationary location) and the response location along the walking path in close proximity to the peak mode amplitude (Murray et al. 2016). A resonant build-up factor is considered to account for the walking path.

SCI P354

SCI P354 (Smith et al. 2009) gives guidance to assess the vibration serviceability of composite steel-concrete floors. SCI P354 response calculation used in this paper is demonstrated in Fig.2. Mode superposition is suggested to obtain the total vibration response under stationary walking at locations of maximum likely response, with mode amplitudes of multiple modes being extracted from the FE model to predict response.

The cut-off frequency between LFF and HFF is 10 Hz; above this limit the floor is assumed to undergo transient response under impulsive footfall loading. For LFFs, the vibration response is determined from contribution of modes up to 12 Hz and is assessed based on a single peak value, which is defined in terms of a R factor. The R factor is the peak of the running root-mean-square

(rms) acceleration for 1 second integration (termed as maximum transient vibration value, MTVV) divided by the reference value of 0.005 m/s^2 (ISO10137 2007). This value may then be evaluated against recommended tolerance limits for different floor functions.

From a practical point of view, a reduction factor ρ (Eq.1) may be applied to the peak rms value to take into account the effect of resonant build-up for a specific walking path. This reduction factor seems to be incorrectly written in this guideline (Davis 2008). The correct form should include the harmonic number term "H_n", as shown in Eq. 2.

$$\rho_{SCI,incorrect} = 1 - e^{-2\pi\zeta f_p \frac{L}{v_p}} \tag{1}$$

$$\rho_{correct} = 1 - e^{-2\pi\zeta H_n f_p \frac{L}{v_p}} \tag{2}$$

HiVoSS

Research Fund for Coal and Steel (RFCS) has published HiVoSS (RFCS 2007b; RFCS 2007a) for vibration design of steel structures. Specifically, this guideline is for composite steel-concrete floors under walking-induced vibration. It is applicable only for floors with natural frequency less than 10 Hz (Sedlacek et al. 2006; Feldmann et al. 2009), even though it is not stated explicitly within the guideline document (e.g (RFCS 2007b)).

HiVoSS approach for response calculation used in this paper is summarized in Fig.3. This guideline treats individual modes from an MDOF system with multiple modes of vibration as individual SDOFs and hence the response of each mode is determined separately and combined using the square-root-sum-of-squares (SRSS) approach. However, it is not clear how many modes should be included when the contributions of all modes are combined.

One-step root-mean-square (OS-RMS) is used as the vibration descriptor, which is a weighted velocity response computed from a combination of pacing frequency and body mass. The OS-RMS multiplied by a factor of 10 gives an equivalent R factor (RFCS 2007b). Vibration tolerance limits are defined for different floor classes and assessment is made against these limits. The HiVoSS

document states that limits specified in ISO10137 (ISO10137 2007), which are used as a basis for limits in SCI P354, CCIP-016 and CSTR43 App G, are "unnecessarily harsh" and proposes limits that are much higher, for example OS-RMS upper limit of 3.2 for offices (equivalent to R=32).

CCIP-016

CCIP-016 (Willford and Young 2006) is applicable for all types of floors and footbridges. This guidance's approach for response calculation implemented in this paper is summarized in Fig.4. Response calculations, similar to other guidelines, are separated into resonant response, for LFFs whose natural frequency is less than 10 Hz, and impulsive response for HFFs above 10.5 Hz. However, it is stated that if the structure is "potentially susceptible to both resonance and impulsive response", both calculation methods should be used and the highest response should be selected for assessment.

The vibration response is determined from contribution of all modes up to 15 Hz and is expressed as a maximum value of rms acceleration with integration time of $1/f_p$. Then, the R factor is computed from the peak rms acceleration, as mentioned before. Similar to SCI P354, a reduction factor is introduced to take into account the resonant build-up of vibration. The R factor is then compared against tolerance limits for various types of floor usage.

CSTR43 App G

CSTR43 App G (Pavic and Willford 2005), similar to CCIP-016, is versatile in its use in terms of construction materials for floors. The response calculation is separated based on the fundamental natural frequency. The threshold frequency is 10 Hz between LFFs and HFFs, which corresponds with resonant and transient response, respectively.

CSTR43 App G approach for response calculation implemented in this paper is summarized in Fig.4. The vibration response is computed, similar to SCI P354, from all modes up to 12 Hz and the resonant reduction factor is applied similar to the aforementioned procedure. Thus, the evaluation is based on a single peak value of R-factor with corresponding recommended limits.

Nature of Forcing Functions Used in Design Guides

The aforementioned design guidelines use deterministic forcing functions based on either Fourier series or polynomial expressions. These are compared in Fig. 5, which shows the forcing functions of each guideline overlaid and normalised by the human body weight. It can be seen that, with the exception of HiVoSS, the various guidelines result in quite similar forcing functions. The HiVoSS forcing function is something of an outlier, with peak force amplitude much larger than those from the other guidelines. None of the guidelines has forcing functions that incorporate the random variability of walking that is observed in real human pedestrians (Brownjohn et al. 2004) due to the "narrow band random process" of walking which has energy at all frequencies (Feldmann et al. 2009).

Most of the above guidelines make a distinction between LFFs, which exhibit primarily resonant response to multiple footfalls at a pacing frequency f_p, and HFFs, which exhibit primarily a transient response to individual footfalls. However, when carrying out a detailed analysis of the performance of the CSTR43 App G guidelines, Zivanović and Pavic (2009) highlighted that there is a 'grey region' between the LFF and HFF thresholds, where both resonant and transient responses contribute to the overall response. This implies that the cut-off frequency and separation of floors based on their fundamental natural frequency may be an unwarranted assumption and a universal forcing function might be a better approach. This was also examined in detail by (Brownjohn et al. 2016), who proposed a response spectrum approach valid for both LFFs and HFFs.

EXPERIMENTAL FLOORS AND FE ANALYSIS

This section presents the experimental data and analytical modeling of three full-scale floors. All of these exhibited a perceptible level of vibration in service and one of these had also provoked adverse comments from occupants over the excessive vibration magnitude. For each tested floor, a detailed FE model was developed to facilitate response prediction using methodologies from each of the aforementioned design guidelines. Experimental modal analysis (EMA) was also performed on each floor to provide experimental modal parameters, which were used to update the FE model. The reason to tune the analytical modal properties to the measured ones was to

eliminate inaccurate FE modelling as a source of error in the evaluation of vibration serviceability; therefore, the analysed floors were verified against measurement data. In addition, walking response measurements were carried out during the experimental campaign to determine the actual vibration response for comparison with the numerical response predictions.

Floor Structure 1 (FS1)

Description of the Floor

FS1 is a floor structure within a recently constructed multi-storey office building, which has an open-plan layout. The details of this floor were presented in detail by (Hudson and Reynolds 2014) and are summarised here for completeness. The floors are of steel-concrete composite construction, within a steel building frame of irregular geometry. Primary beams (girders) have spans of up to 10 m, secondary beams (beams) are at 3 m spacing with spans up to 13 m and steel columns lie roughly on a typical grid of 13 m $\times$ 9 m, as shown in Fig. 6.

Construction drawings were used to determine the size of structural members. A 130 mm thick light weight concrete is poured upon a 60 mm trapezoidal steel profile decking to form the floor slab, which acts compositely with the secondary beams. Details of the structural elements vary due to the irregular geometry, but in a typical bay secondary beams are cellular with asymmetric form. The section sizes are lower tee 610×229×113 UB and upper tee 457×191×89 UB, with hole diameter of 500 mm at 750 mm centres. Primary beams are 792×191/229×101 ACB sections and column members are 254×254×73 UC. There are three reinforced concrete core walls to provide lateral resistance to the whole structure; these have been included in the FE model due to their significant effect on the structural modes.

Experimental Modal Analysis (EMA)

Experimental modal properties of the floor were determined from in-situ modal testing using multi-reference uncorrelated random excitation from four APS Dynamics shakers (2× APS113 and 2× APS400) and a test grid of roving accelerometers (Honeywell QA750), as shown in Fig. 7. Frequency response functions (FRFs) were acquired using a Data Physics Mobilyzer DP730 digital spectrum analyser, and polyreference FRF curve fitting was utilized to determine the experimental

modal properties. The ME'scope suite of modal parameter estimation software was used to extract modal properties using a multi-polynomial method to provide reliable estimates of mode frequency, damping and shape. The final mode shape results are shown in Fig. 8.

Development of FE model and Analysis

The structural members were modeled in ANSYS. The composite steel-concrete floor was modeled using SHELL181 elements and orthotropic properties were assumed (flexural stiffness in the direction of the ribs is higher than the perpendicular direction). Beams and columns were modeled using BEAM188 elements. The composite action between the beams and slabs was modeled through a vertical offset of the shell element as recommended in the design guidelines (Willford and Young 2006; Smith et al. 2009). The modulus of elasticity (E) of 22 GPa for lightweight concrete and density of 1800 kg/m^3 were assumed (Pavic and Willford 2005). A modal analysis was carried out to obtain modal frequencies, mode shapes and modal masses.

Updating the FE model using manual tuning was conducted by introducing a full height partition wall modeled using SHELL181 elements with assumed E of 5 GPa and density of 2500 kg/m^3 between gridline 5D-5E. Also, sensitivity analysis was conducted to obtain the most appropriate parameters of E and density of both concrete and steel. After modal updating, the final values that gave a close match to the measured modes were 24 GPa and 210 GPa for E of concrete and steel, respectively. Material density of steel was 7830 kg/m^3 and concrete 1800 kg/m^3, as determined from the literature. Analytical FRF plots were also produced to compare and reconcile with those from the measured data, as demonstrated in Fig.9. To generate these FRF plots, a level of damping ratio had to be assumed from guidelines suggestion. The value chosen for this floor was 3% based upon guideline recommendations for all modes. It is apparent that, despite matching the mode shapes quite well, the FE FRF does not match very well with the measured FRF. However, the modal assurance criterion (MAC), shown in Fig.8 and Table 1, exhibits a good consistency. This might be associated with some of the difficulties related to modeling civil engineering floor structures, where uncertainty in modeling parameters may affect the accuracy of the FE model.

Floor Structure 2 (FS2)

Description of the Floor

This is the second case-study floor, which has the longest span of all three cases. This floor was tested at its bare stage (construction stage). It is a steel-concrete composite floor with normal weight concrete poured into a 130 mm deep slab. Secondary beams span 15 m at a spacing of 3.125 m. The primary beams have a span of 6.25 m. The columns are situated at the intersection of beams, with typical bay sizes of 15 m × 6.25 m, as shown in Fig. 10. Details of the structural elements in a typical bay are; secondary beams are cellular section sizes 720.5×152/229×81 UB, with hole diameter of 500 mm at 750 mm centres. Primary beams are 762×267×134 UB and column members are 305×305×158 UC. There are two reinforced concrete walls with 300 mm thickness for lateral resistance.

Experimental Modal Analysis (EMA)

A modal test was performed using two APS Dynamics Model 400 electrodynamic shakers as excitation sources. The structural response was measured using Honeywell accelerometers (model QA750). Digital data acquisition was performed using a portal spectrum analyzer model Data Physics DP730, similar to FS1. The analyzer provides immediate calculation of the FRFs so that the quality of measurement data can be checked during the test. The measurements were acquired over a test grid of 93 test points, as shown in Fig. 11. These test points were utilized to acquire the modal properties between gridelines F and O.

Similar to FS1, the ME'scope suite of modal parameter estimation software was used to extract the modal properties shown in Fig. 12.

FE Analysis

The ANSYS FE software was utilized to model all components of the floor structure. Orthotropic properties were applied to the SHELL181 elements to model the floor slab with vertical offset to incorporate composite action. All beams and columns were modeled as BEAM188 with both their ends assumed to have rigid connections (Smith et al. 2009). Due to the construction stage and uncompleted top floor (there was only steel deck and partial beam members with no concrete),

COMBIN40 was used to model the vertical constraint of "discontinuous columns" in Fig.10. COMBIN40 is a single degree of freedom (SDOF) mass/spring element in ANSYS, which mass (M) and stiffness (K) were assigned. Since there was no concrete at that floor, COMBIN40 tends to behave as a connection for top columns during modal analysis.

The initial model required a number of updating iterations to reconcile with the measured modal analysis and hence manual model updating was conducted for global parameters. The parameters updated were E and density of concrete and steel, COMBIN40 properties, lateral bracing members and partition wall installed beneath the exterior frame. After modal updating, the final values that gave a good reconciliation with measured modes were 37 GPa and 210 GPa for E of concrete and steel, respectively. The material density of steel was 7830 kg/m^3 and that of concrete was 2300 kg/m^3. Concrete block masonry of 150 mm thick with E of 22 GPa and density of 2000 kg/m^3 were assumed. COMBIN40 parameters were K=12500 N/m and M=15000 kg. It is worth noting that partition walls beneath the exterior frame had a significant effect on the mode sequences and family of modes; therefore, their modeling improved significantly the FE model. These values provided good matching with measured results and thus it can be considered as reliable. Predicted modal frequencies and mode shapes are illustrated in Fig. 12. A damping ratio of 1% was assumed for FRF generation based on the recommendations for bare floors. Analytical and experimental FRFs are shown in Fig. 13. It is obvious that there is a good matching between the two FRFs, albeit with some inconsistencies. Also, the modal assurance criterion (MAC), presented in Table 2, exhibits a good consistency; this indicates the FE model is comparably reconciled with the experimental data.

Floor Structure 3 (FS3)

Description of the Floor

This test structure is the second floor in a four-storey multi-purpose building. It is fully furnished composite steel and concrete floor spanning 9.754 m between gridlines H to C and 6.09 m between gridlines 24 to 30 (Fig. 14). Steel decking supports the in-situ cast normal weight concrete slab, which spans in the direction orthogonal to the secondary beams. At the time of testing, mechanical services and raised flooring were mounted beneath and on top the floor. The slab thickness varied from 150 mm to 200 mm due to refurbishments. The shaded area in Fig.14 indicates an area which was originally intended to be a swimming pool, but was never used for this purpose. In this area the slab thickness is 200 mm and there is additional mass loading from demolished partition walls that were used bring the floor surface up to the same level as the rest of the floor.

Secondary beams in a typical bay are 457×152×60 UB, whereas primary beams are 533×210×92 UB. Column members are 254×254×89 UC and bracing members are 193.7×12.5 CHS. Lateral stiffness is provided by the bracing members along the edges of the structure.

Experimental Modal Analysis (EMA)

Natural modes were estimated for this floor using EMA with four electrodynamic shakers and an array of response accelerometers in the same was as described for FS1. FRF measurements were made over a test grid of 81 points, as shown in Fig. 15, using a portable spectrum analyzer. To estimate modal properties curve fitting of the FRF data was carried out using the ME'scope parameter estimation software. In-service monitoring was carried out on this floor for a duration of 12 hours under normal operation, which provided the actual vibration performance of the floor.

FE Analysis

Model of the structure was developed in the ANSYS FE software. Floors were modeled using SHELL181 elements, whereas beams and columns were modeled using BEAM188 elements. Orthotropic properties were assumed for the floors. The shaded area in Fig. 14 was modeled using SOLID165 elements, which is an element to model volumes and it is used for the volume of the additional mass of the intended swimming pool.

Initial modeling did not result in good matching and as such the top floor together with some substantial full height partition walls, were added to the model. This led to a better matching of mode shapes in terms of frequency and mode sequences, as shown in Fig. 16. Similar to the two previous case-study floors, manual updating was used to update the FE model. The updating process progressed by altering floor material properties such as density and E, as well as properties related to the partition walls. The model resulted in closely-spaced modes due to repetitive geometry and orthotropic properties, which is expected in floors (Pavic et al. 2008). Modal frequencies and mode shapes are shown in Fig. 16. The FE mode shapes shown are for the considered floor and top level floor is excluded, for illustration purposes. FRF plots were generated from FE modeling to display the matching trend with experimental data at shaker points. Fig. 17 shows the analytical and experimental FRFs at four shaker locations. Damping ratio of 3% was assumed based on the guideline suggestions for office floors. The MAC values in Fig.16 and Table 3 show to an extend a good match and the analytical FRF plots seem to correlate with those of measurements and thus the FE model appears to be realistic. This is a clear indication of the need to include partition walls and top floors in the model when carrying out evaluation of vibration responses.

EVALUATION OF RESPONSE PREDICTION USING GUIDELINES

Pre-construction: Design Stage

This sections presents the evaluation of response using each of the guidelines to calculate modal properties, vibration responses and applying the recommended evaluation procedures.

Modal Properties Estimation

- **FS1:** FS1 has an irregular plan configuration except for a few bays, to which the simplified formulae of the guidance are somewhat applicable. Hence, modal properties are determined for floor bay C2-D3 (see Fig. 6). Methodologies and simplified equations or recommended values provided by each guideline are utilized to estimate the dynamic properties shown in Table 4. CSTR43 App G does not provide any simplified techniques and as such formulae given in structural dynamics textbooks (e.g. (Smith 1988) or (Blevins 1979)) have been

used. Similar formulae are also applicable to the other case study floors.

- **FS2:** Modal properties are determined for a typical floor bay L1-M5 (see Fig. 10), since the floor is regular and the dimensions of most bays are the same. Simplified equations and recommended values provided by each guideline are utilized to estimate the dynamic properties, shown in Table 5.
- **FS3:** Modal properties are determined for a typical floor bay F29-E28 (see Fig. 14), due to regular plan of the floor. Simplified equations and recommended values provided by each guideline are utilized to estimate the dynamic properties, shown in Table 6.

Response Prediction

Prediction of vibration responses in this paper using both FE analysis and hand calculations is based on the methodology of each guideline as illustrated in Figs.1,2,3 and 4. When using FE analysis, mode coordinates are extracted for excitation and response points. Contribution of more than one mode is then combined through a mode superposition approach. The guidelines that utilize such method are SCI P354, CCIP-016 and CSTR43 App G.

AISC DG11 suggests using harmonic analysis; a typical FRF plot from this analysis is shown in Fig.18 for FS1. HiVoSS assumes each vibration mode from FE analysis as a SDOF and as such the response is calculated from each mode and superimposed using SRSS. In addition, HiVoSS provides charts of vibration response, where the response can be read off from a known modal properties. It is worth mentioning that none of the guidelines defines walking routes, nor do they pay attention to non-stationary nature of pedestrians. However, it is speculated to take into account the line of strongest response (maximum modal ordinates) or mode amplitudes close to, where possible, a predefined "walking path". Such method may yield an assumption of exciting the highest mode amplitudes in order to obtain conservatively the uppermost response. It is indicated (Zivanović et al. 2012) that significant inaccuracies occur due to the presence of variations in walking loads and uncorroborated assumptions in response estimation.

As far as manual calculations are concerned, the guidelines follow simple techniques to predict the vibration response. This typically includes estimating modal properties of the fundamental

mode, assuming a harmonic walking load and thus predicting the response. It is worth noting that the simplified techniques can estimate accurately the modal frequency, yet an incorrect modal mass is often obtained. The vibration response can be significantly affected by such inaccuracies in modal properties and more importantly the estimation of the modal damping.

Here, the vibration responses are calculated based on the above procedure from both the FE analysis and manual calculations for the case study floors, as shown below.

- **FS1**: This is a relatively new office floor, where pedestrians use various paths during normal operations. Although floor occupants had not reported any adverse comments, perceptible vibration was obvious and thus the floor can be considered as a "borderline" case. The predicted vibration responses following procedures in each guideline are shown in Fig.19. It can be seen that the predicted responses vary significantly and hence the vibration serviceability assessment can be inconclusive. In particular, use of the simplified procedures for modal parameter estimation seem to be inaccurate for estimation of floor performance. Also, the assumption of steady state vibration response for serviceability assessment is another potential source of inaccuracy, although the measured responses can vary due to the variations in subjects' excitation and modal properties. Reynolds and Pavic (2015) remark that use of peak responses is potentially overconservative, whereas using vibration dose values or cumulative distribution of response might provide more reliable assessment.
- **FS2**: This floor is a multi-purpose floor, used as a wedding venue, for meetings and as a leisure center. During construction the floors had been reported to be highly responsive, which raised concerns of the construction contractor. The predicted vibration response compared with the measured response is shown in Fig.20. A good prediction is obtained via AISC DG11 methodology in terms of equivalent R-factor, whereas the rest of the guidelines are dissimilar and diverse. Due to the relatively regular plan configuration, both the simplified formula and FE methodology seem to work well per AISC DG11. There are large overestimations by most guidelines, which dictate neither satisfactory or unsatisfactory con-

dition. Such discrepancies indicate the necessity for significant improvements in response prediction and tolerance limits to facilitate reliable and realistic ratings at the design stage.

- **FS3**: This floor is also an office floor, which is mostly used as a library and study area. The floors had been reported to exhibit large vibration responses during in-service operation, due to the gymnasium operating on the floor above, and thus the floor occupants expressed annoyance over the magnitude of vibration. The predicted response and its measured counterpart are shown in Fig.21. The significant underestimation of response observed for all guidelines is due to the difference between the loading condition assumed (i.e. single person walking) and the actual loading condition (one or more people exercising in the gymnasium above) and hence cannot be attributed to lack of performance of the guidelines. Nevertheless, this case does demonstrate an alternative loading mechanism that should be considered in buildings with multiple types of occupation.

Assessment Criteria

- **FS1**: As indicated in Fig.19, this office floor has unacceptable performance according to CSTR43 App G and CCIP-016, but it is deemed satisfactory and within allowable limits (recommended floor classes in HiVoSS) with respect to AISC DG11, SCI P354 and HiVoSS. As a consequence, the assessment of the floor under walking is not clearly predicted.
- **FS2**: Due to the multi-functional purpose of this structure, its performance might be evaluated against a range of assessment criteria. However, in this case it is evaluated against the assessment criteria for an office floor, which is also reasonable for a meeting venue. Fig.20 shows the response assessed against the relevant threshold limits. It is apparent that the floor is unacceptable according to four of the guidelines, whereas it satisfies the requirements of HiVoSS for such structures.
- **FS3**: Similar to FS1, this floor is assessed under office floor requirements. It is shown in Fig.21 that it performs well for all guidelines. Whilst the problem with this floor was due to high levels of rhythmic excitation coming from the floor above, it can be seen that for normal office walking the floor would have been expected to perform satisfactorily. This

correlated with subjective assessment made during the testing.

Post-construction: In-service Condition

- **FS1**: The actual response presented in Fig.19 is measured under a single person walking via the walking path (WP) in Fig.6. It is clear that this floor has a satisfactory level of vibration, despite being perceptible. In addition, field monitoring indicated that the level of vibration did not reach the level of human discomfort. The actual vibration response (red line) corresponds to an R-factor of 5.3 for which floor occupants had a perceptible vibration without complaining. Hence, from standpoint of normal operation this floor can be considered as acceptable.
- **FS2**: The actual vibration response under a single person walking resulted in an R-factor of 8.2, as shown in Fig.20. Although it is predicted to be unacceptable, the actual response was measured along the walking path (WP) shown in Fig.10. It is clear that the predicted responses are scattered around the measured R-factor. As mentioned in previous section, AISC DG 11 seems to be in close proximity to the actual response. However, it is difficult to carry out a reliable assessment due to the diverse predictions of the various guidelines.
- **FS3**: It is shown in Fig.21 that this floor had very high level of in-service response, which resulted in complaints from floor occupants about the vibration. The measured R-factor in service reached 15.1 under excitation from the gymnasium above. Whilst it is not possible to draw any conclusions about the performance of the guidelines in terms of predicting the response, it is possible to assess whether the response criteria are appropriate. Examining Fig.21, it can be seen that the tolerance limit of the HiVoSS guideline was more than double the measured R-factor, and hence it would be predicted to be acceptable. This clearly was not the case since significant complaints had been received from the building occupants. The rest of the guidelines produced an assessment that the floor is unacceptable, which correlates with the subjective assessment.

RESULTS AND DISCUSSION

From the analyses presented in this paper, it is clear that the various available design guidelines do not give a consistent prediction of the vibration serviceability performance of the floor structures considered.

The results of the maximum predicted R factor for all three case-studies show that the guidelines predict quite different values of R-factor or equivalent. There are contradictory response predictions between CCIP-016, CSTR43 App G and SCI P354 when comparing the same vibration metric. AISC DG11 performs relatively well in terms of both response prediction and assessment for FS1 and FS2 and also gave a clear assessment of FS3 as being highly unsatisfactory, as expected. HiVoSS, however, appears to be an outlier and highly inaccurate.

None of the guidelines was able to give any insight into the frequency of event occurrence. A single peak value compared against the available tolerance limits may not be representative of the actual in-service condition, if this condition occurs only very rarely. This may lead to inconsistencies between the design stage assessment and actual performance in service. Such a wide discrepancy can cause confusion for design engineers as to whether the vibration performance is satisfactory or not. Another matter that could arise is the question of what is the probability of occurrence of the above predictions? In some cases, these guidelines can produce responses close to those measured on the actual structure, but it is not clear for any particular structure at the design stage whether there might be over- or under-estimation.

Simplified techniques for estimation of modal parameters giving results previously shown produce large differences in modal mass values, whereas modal frequency seems to be relatively well predicted. All guidelines tend to consider modal mass differently. As such, even larger inaccuracies appear to occur in obtaining the modal mass, which lead to potentially inaccurate estimations of vibration response. Such discrepancies in modal mass highlights that the simply-supported plate theory and empirically adjusting for a bay geometry (i.e span and width) can produce misleading values, even for regular floor configurations. This has also been observed in (Middleton 2009). It is worth noting that the recommended damping ratios for the case-study floors seem to be somewhat in line with the measurements.

These case-study floors have illustrated a number of major drawbacks in contemporary guidelines in computing vibration response to pedestrian excitation. These are the simplified formulae which inaccurately estimate the modal properties and hence produce inaccurate estimates of response. The lack of a realistic vibration response descriptor with respective tolerance limits may also be a major downside in these guidelines; a single peak value of vibration response appears to be unrepresentative. Therefore, significant improvements are needed with respect to dynamic properties, expected loading scenarios and the corresponding walking-induced forces. This would result in a more reliable vibration response, which might be in the form of probability of exceedence with a realistic predefined set of values for serviceability assessment. This approach would not only give design engineers a reliable tool, but also provide a realistic response estimate for various floor usage scenarios; thus, leading to more reliable vibration serviceability assessment of floor structures.

CONCLUSION

This paper has presented a back analysis of contemporary design guidelines using three floors that were also physically tested. The merits and demerits of the guidances have been illustrated and examined. Vibration serviceability assessment has been performed based on the tuned FE model for all floors as well as the respective simplified formula has been used. Vibration responses were calculated for a range of the floor frequencies to obtain the peak vibration response in terms of equivalent R-factor (for peak acceleration and OS-RMS$_{90}$) for the guidelines due to ease of comparison.

Walking load models are represented either by Fourier series or a polynomial function. These are periodic modeling of a single person without considering the innate variabilities of actual walking and as such a probabilistic walking load model remains absent. The frequency threshold between LFFs and HFFs is the key factor to determine vibration responses (resonant response to multiple footfalls or transient response to individual footfalls) that govern the design procedure. The methodologies presented in each guidelines predict a vibration response that may or may not match well with actual measurements. A significant over- and under-estimation can be seen in all

guidelines, which can be attributed mainly to inaccurate estimation of modal properties, particularly for the simplified procedures.

A steady state response value appears to be misleading and unrepresentative for vibration serviceability assessment. Identifying an appropriate vibration descriptor (including tolerance limits) coupled with a probabilistic framework might be a key factor for more reliable serviceability assessment. In addition, conservative design with an accept-reject method neither results in a reliable assessment, nor describes the rare vibration events that may happen. Therefore, significant improvements and rigorous approaches are required to introduce probability of exceedence with realistic predefined set of values. The vibration ratings and tolerance limits should also reflect such a statistical manner. This approach would not only give design engineers a reliable tool, but may also lead to more reliable vibration serviceability assessment of floor structures.

ACKNOWLEDGEMENTS

The financial support for this research was provided by Qatar National Research Fund (QNRF; a member of the Qatar Foundation) via the National Priorities Research Program (NPRP), Project Number NPRP8-836-2-353 . The statements made herein are solely the responsibility of the authors.

REFERENCES

Blevins, R. (1979). *Formulas for natural frequency and mode shape*. Litton Educational Publ., Inc, New York.

Brownjohn, J., Pavic, A., and Omenzetter, P. (2004). "A spectral density approach for modelling continuous vertical forces on pedestrian structures due to walking." *Can. J. Civ. Eng.*, 31(1), 65–77.

Brownjohn, J., Racic, V., and Chen, J. (2016). "Universal response spectrum procedure for predicting walking-induced floor vibration." *Mech. Syst. & Signal Process.*, 71(1), 741–755.

Davis, D. B. (2008). "Finite element modeling for prediction of low frequency floor vibrations due to walking." Ph.D. thesis, The Virginia Polytechnic Institute and State University, Blacksburg, Virginia, USA.

Fanella, D. A. and Mota, M. (2014). *Design guide for vibrations of reinforced concrete floor systems*. Concrete Reinforcing Steel Institute (CRSI), Schaumburg, IL.

Feldmann, M., Heinemeyer, C., Butz, C., Caetano, E., Cunha, A., Galanti, F., Goldack, A., Helcher, O., Keil, A., Obiala, R., Schlaich, M., Sedlacek, G., Smith, A., and Waarts, P. (2009). "Design of floor structures for human induced vibrations." *Joint Rep EUR 24084 EN*, European Commission-JRC, Luxembourg.

Hassan, O. A. B. and Girhammar, U. A. (2013). "Assessment of footfall-induced vibrations in timber and lightweight composite floors." *Int. J. of Struct. Stability & Dyn.*, 13(2), 1–26.

Hudson, E. J. and Reynolds, P. (2014). "Implications of structural design on the effectiveness of active vibration control of floor structures." *Struct. Control & Health Monit.*, 21(5), 685–704.

ISO10137 (2007). *Bases for tesing o f structures- serviceability of buildings and walkways against vibrations*. Geneva, Switzerland.

Liu, D. and Davis, B. (2015). "Walking vibration response of high-frequency floors supporting sensitive equipment." *J. of Struct Eng*, 141(8), 1–10.

Middleton, C. J. (2009). "Dynamic performance of high frequency floors." Ph.D. thesis, The University of Sheffield, Sheffield, UK.

Muhammad, Z., Reynolds, P., and Hudson, E. (2017). "Evaluation of contemporary guidelines for floor vibration serviceability assessment." *Dyn. of Civ. Struct., Vol. 2 : Proc. of the 35th IMAC, A Conf. and Expos. on Struct. Dyn. 2017*, Springer Int. Publ., 339–346.

Murray, T. M., Allen, D. E., Ungar, E. E., and Davis, D. B. (2016). *Vibrations of steel-framed structural systems due to human activity*. American Institute of Steel Construction (AISC), USA.

Nguyen, H. A. U. (2013). "Walking induced floor vibration design and control." Ph.D. thesis, Swinburne University of Technology, Australia.

Pavic, A., Miskovic, Z., and Živanović, S. (2008). "Modal properties of beam-and-block pre-cast floors." *The IES J. Part A: Civ. & Struct. Eng.*, 1(3), 171–185.

Pavic, A. and Willford, M. (2005). *Vibration serviceability of post- tensioned concrete floors*. Concrete Society, Slough, UK, 2nd edition.

Reynolds, P. and Pavic, A. (2003). "Effects of false floors on vibration serviceability of building floors. i: Modal properties." *J. of Perform. of Constr. Facil.*, 17(2), 75–86.

Reynolds, P. and Pavic, A. (2015). "Reliability of assessment criteria for office floor vibrations." *50th U.K. Conf. on Hum. Responses to Vib.*, Southampton, UK.

RFCS (2007a). *Human induced vibrations of steel structures (HiVoSS) -vibration design of floors: background documnet*. European Comission-RFCS, Brussels, Belgium.

RFCS (2007b). *Human induced vibrations of steel structures (HiVoSS) -vibration design of floors: guideline*. European Comission-RFCS, Brussels, Belgium.

Sedlacek, G., Heinemeyer, C., Butz, C., Volling, B., Waarts, P., Van Duin, F., Hicks, S., Devine, P., and Demarco, T. (2006). "Generalisation of criteria for floor vibrations for industrial, office, residential and public building and gymnastic halls." *Tech.Rep Eur 21972 EN*, European Commission-JRC, Luxembourg.

Setareh, M. (2009). "Vibration serviceability of a building floor structure. ii: Vibration evaluation and assessment." *J. of Perform. of Constr. Facil.*, 24(6), 508–518.

Smith, A., Hicks, S., and Devine, P. (2009). *Design of floors for vibration: A new approach*. Steel Construction Institute (SCI), Berkshire, UK, 2nd edition.

Smith, J. (1988). *Vibration of structures. Application in civil engineering desing*. Chapman & Hall, London, England.

Willford, M. and Young, P. (2006). *A Design guide for footfall induced vibration of structures*. Concrete Centre(CC), Surry, UK.

Zivanović, S. (2006). "Probability-based estimation of vibration for pedestrian structures due to walking." Ph.D. thesis, The University of Sheffield, Sheffield, UK.

Zivanović, S. and Pavic, A. (2009). "Probabilistic modeling of walking excitation for building floors." *J. of Perform. of Constr. Facil.*, 23(3), 132–143.

Zivanović, S., Pavic, A., and Racic, V. (2012). "Towards modelling in-service pedestrian loading of floor structures." *Dyn. of Civ. Struct., Vol. 1 : Proc. of the 30th IMAC, A Conf. and Expos. on Struct. Dyn. 2012*, Springer Int. Publ., New York, NY, 85–94.

577 Zivanović, S., Pavic, A., and Reynolds, P. (2007). "Probability-based prediction of multi-mode
578 vibration response to walking excitation." *Eng. Struc.*, 29(6), 942–954.

List of Tables

1 MAC values FS1 25

2 MAC values FS2 26

3 MAC values FS3 27

4 Modal properties of FS1 from design guidance simplified formulae 28

5 Modal properties of FS2 from design guidance simplified formulae 29

6 Modal properties of FS3 from design guidance simplified formula 30

TABLE 1. MAC values FS1

		Analytical			
	Mode No.	1	2	3	4
Measured	1	0.9013	0.1214	0.0245	0.1167
	2	0.2162	0.8721	0.027	0.1088
	3	0.026	0.191	0.912	0.16
	4	0.2383	0.1071	0.132	0.8899

TABLE 2. MAC values FS2

		Analytical			
	Mode No.	1	2	3	4
Measured	1	0.989	0.0752	0.0912	0.0599
	2	0.0313	0.942	0.0951	0.099
	3	0.0959	0.0868	0.939	0.142
	4	0.0677	0.107	0.129	0.9125

TABLE 3. MAC values FS3

		Analytical			
	Mode No.	1	2	3	4
Measured	1	0.88	0.117	0	0.129
	2	0.195	0.851		0.282
	3	0	0	0	0
	4	0.142	0.228	0	0.879

TABLE 4. Modal properties of FS1 from design guidance simplified formulae

Guidance	**Natural frequency (Hz)**	**Modal mass (t)**	**Damping ratio (ζ)**
Measured	5.24	36.98	3.16%
AISC DG11	4.99	51	3%
SCI P354	5.23	17.47	3%
HiVoSS	5.18	15.9	3%
CCIP-016	2.89	7.95	3%
CSTR43 App G	4.52	7.95	3%

TABLE 5. Modal properties of FS2 from design guidance simplified formulae

Guidance	**Natural frequency (Hz)**	**Modal mass (t)**	**Damping ratio (ζ)**
Measured	4.92	102.03	0.66%
AISC DG11	4.48	83.6	1%
SCI P354	4.99	17.26	1.1%
HiVoSS	4.78	14.77	1%
CCIP-016	4.1	7.4	1.15%
CSTR43 App G	6.5	7.4	1%

TABLE 6. Modal properties of FS3 from design guidance simplified formula

Guidance	**Natural frequency (Hz)**	**Modal mass (t)**	**Damping ratio (ζ)**
Measured	6.56	93.5	1.0%
AISC DG11	6.03	60.8	3%
SCI P354	6.61	20.98	3%
HiVoSS	6.55	12.4	3%
CCIP-016	5.47	6.2	3%
CSTR43 App G	7.24	6.2	3%

List of Figures

1 AISC DG11 vibration analysis procedure and chapter designation. 34

2 SCI P354 vibration analysis procedure and chapter designation. 35

3 HiVoSS vibration analysis procedure and chapter designation. 36

4 CCIP-016 and CSTR43 App G vibration analysis procedure. 37

5 Comparison between pedestrian forcing functions. 38

6 Plan layout of FS1 39

7 Test point locations on FS1. Excitation locations are shown by letter "S". 40

8 FS1 vibration modes from FE Analysis and Experimental Modal Analysis 41

a FE analysis, f_1 = 5.23 Hz, m = 36.02 tonnes, MAC = 0.90 41

b EMA f_1 = 5.24 Hz, ζ = 3.16 % 41

c FE analysis, f_2 = 6.52 Hz, m = 28.54 tonnes, MAC = 0.87 41

d EMA f_2 = 6.06 Hz, ζ = 2.24 % 41

e FE analysis, f_3 = 6.33 Hz, m = 35.95 tonnes, MAC = 0.91 41

f EMA f_3 = 6.58 Hz, ζ = 1.87 % 41

g FE analysis, f_4 = 6.87 Hz, m = 39.95 tonnes, MAC = 0.89 41

h EMA f_4 = 7.31 Hz, ζ = 1.7 % 41

9 Comparison of experimental FRFs and those from the updated FE model at four locations on FS1 42

a FRF@TP20 42

b FRF@TP32 42

c FRF@TP28 42

d FRF@TP59 42

10 Plan layout of FS2 43

11 Test point locations on FS2. Excitation locations are shown by letter "S". 44

12 FS2 vibration modes from FE Analysis and Experimental Modal Analysis 45

a FE analysis, f_1 = 4.88 Hz, m = 85.15 tonnes, MAC = 0.98 45

b EMA f_1 = 4.92 Hz, ζ = 0.66 % 45
c FE analysis, f_2 = 5.43 Hz, m = 92.89 tonnes, MAC = 0.94 45
d EMA f_2 = 5.51 Hz, ζ = 0.74 % 45
e FE analysis, f_3 = 6.41 Hz, m = 32.02 tonnes, MAC = 0.93 45
f EMA f_3 = 6.12 Hz, ζ = 0.32 % 45
g FE analysis, f_4 = 6.48 Hz, m = 33 tonnes, MAC = 0.91 45
h EMA f_4 = 6.55 Hz, ζ = 0.32 % 45
13 Comparison of experimental FRFs and those from the updated FE model at two locations on FS2 46
a FRF@TP112 46
b FRF@TP310 46
14 Plan layout of FS3 47
15 Test point locations on FS3. Excitation locations are shown by the letter “S”. 48
16 FS3 vibration modes from FE Analysis and Experimental Modal Analysis 49
a FE analysis, f_1 = 6.57 Hz, m = 114.6 tonnes, MAC = 0.88 49
b EMA f_1 = 6.56 Hz, ζ = 1.0 % 49
c FE analysis, f_2 = 6.84 Hz, m = 96.15 tonnes,, MAC = 0.85 49
d EMA f_2 = 6.89 Hz, ζ = 1.04 % 49
e FE analysis, f_3 = 7.23 Hz, m = 104.13 tonnes 49
f EMA f_3 = 0, ζ = 0 % 49
g FE analysis, f_4 = 7.4 Hz, m = 104.53 tonnes, MAC = 0.87 49
h EMA f_4 = 7.39 Hz, ζ = 0.62 % 49
17 Comparison of experimental FRFs and those from the updated FE model at four locations on FS3 50
a FRF@TP29 50
b FRF@TP33 50
c FRF@TP49 50

d FRF@TP53 50
18 Peak FRF magnitude from FE harmonic analysis between grid line B-1 & C-2 . . . 51
19 FS1 Response prediction of guidelines against actual measured response 52
20 FS2 Response prediction of guidelines against actual response 53
21 FS3 Response prediction of guidelines against actual response 54

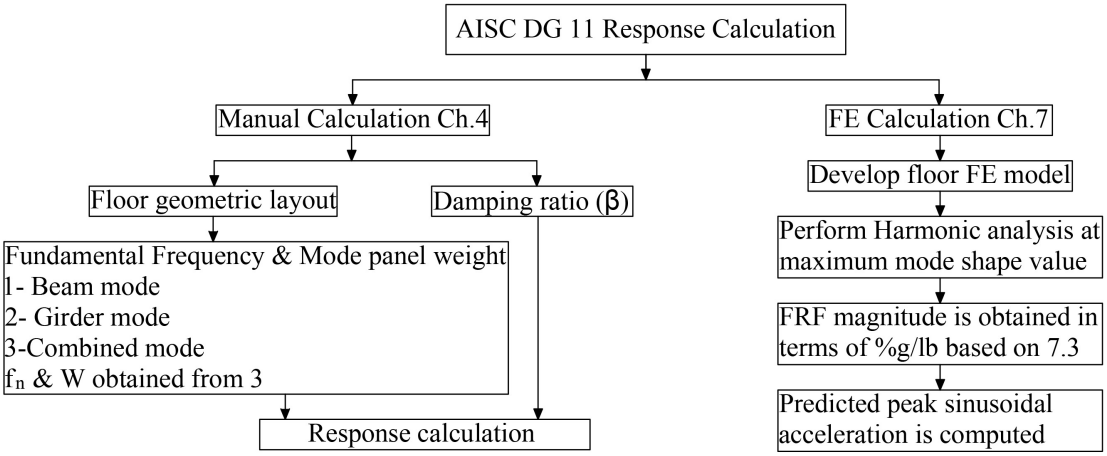

Fig. 1. AISC DG11 vibration analysis procedure and chapter designation.

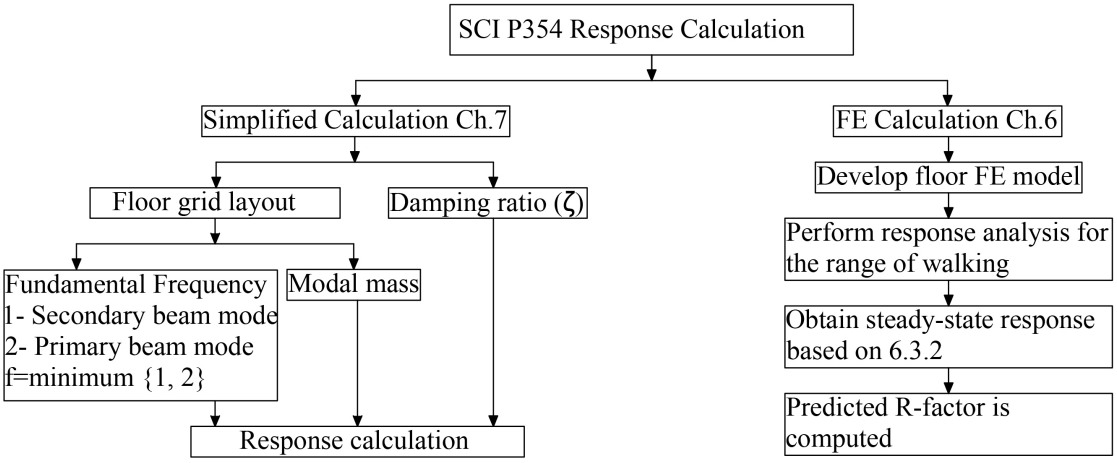

Fig. 2. SCI P354 vibration analysis procedure and chapter designation.

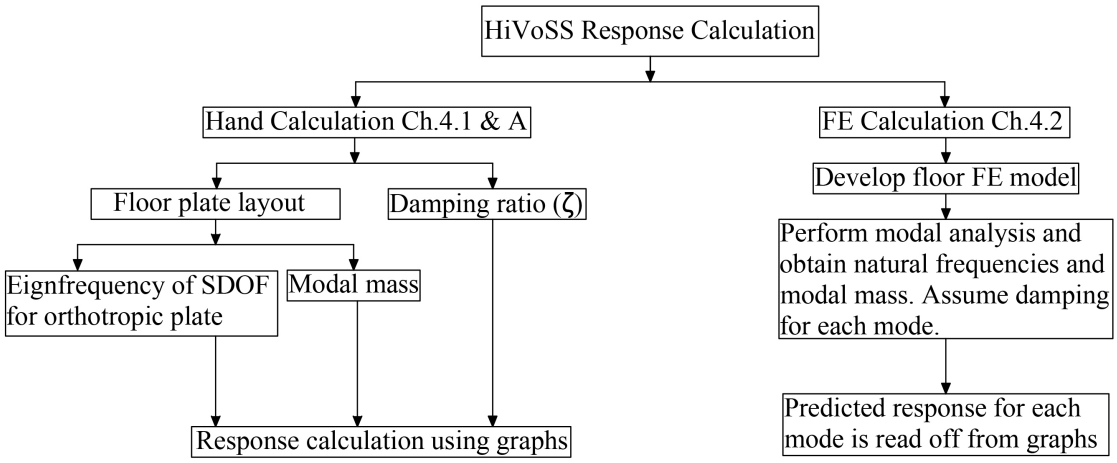

Fig. 3. HiVoSS vibration analysis procedure and chapter designation.

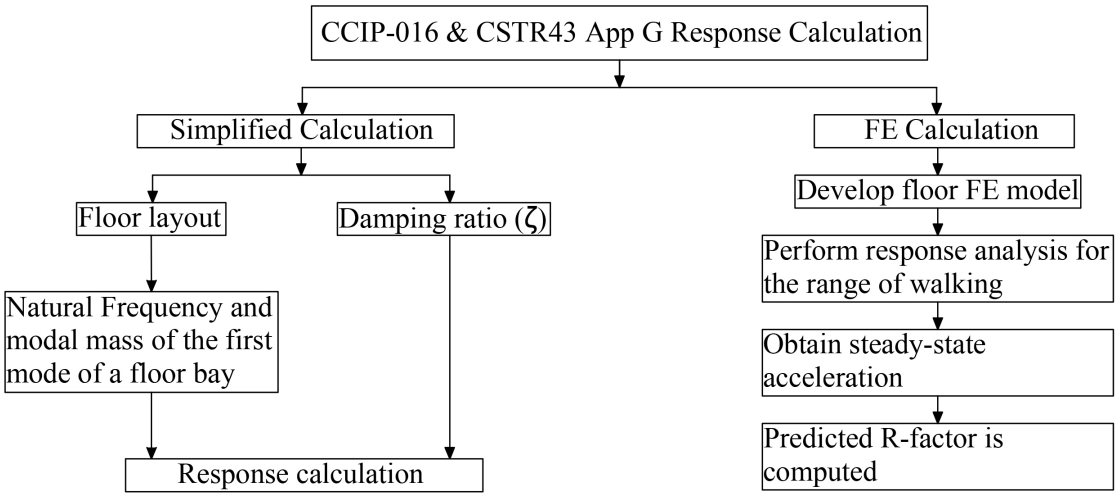

Fig. 4. CCIP-016 and CSTR43 App G vibration analysis procedure.

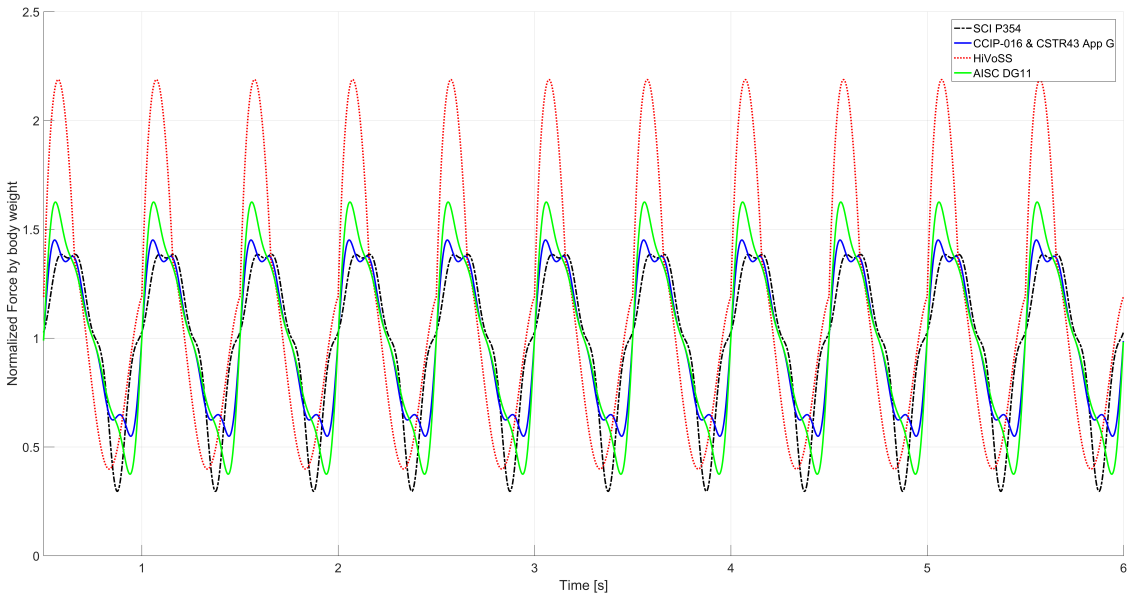

Fig. 5. Comparison between pedestrian forcing functions.

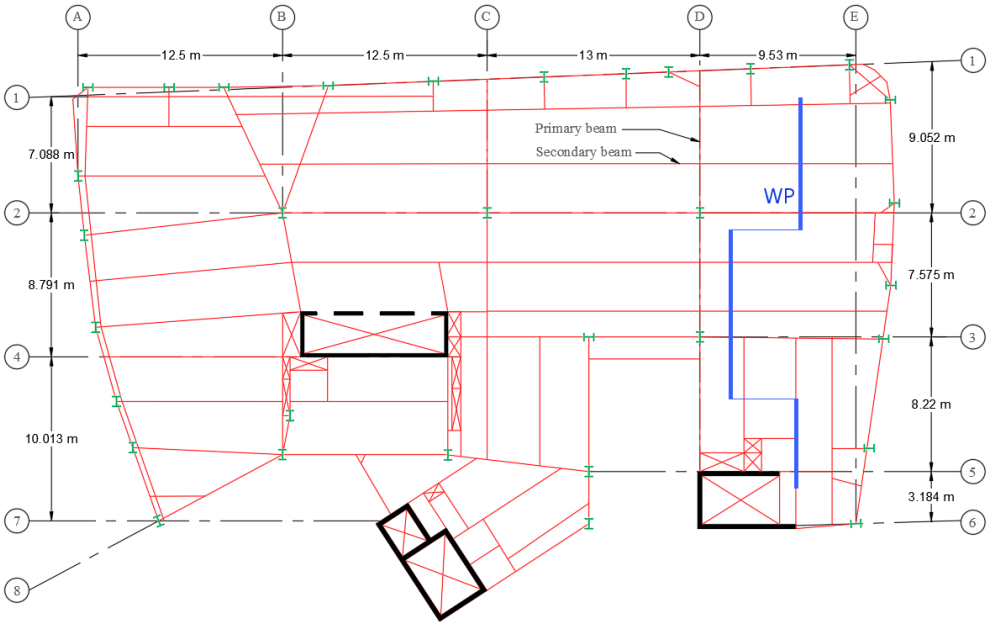

Fig. 6. Plan layout of FS1

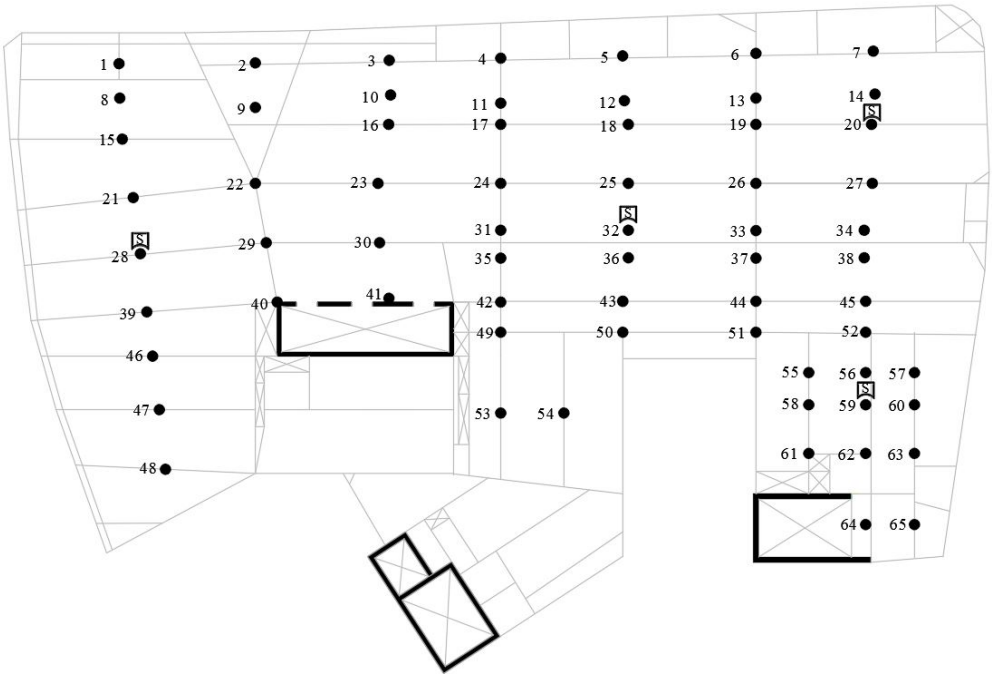

Fig. 7. Test point locations on FS1. Excitation locations are shown by letter “S”.

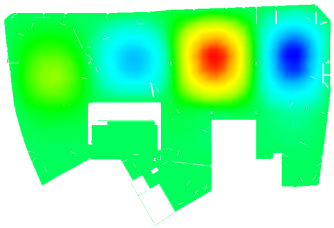

(a) FE analysis, f_1 = 5.23 Hz, m = 36.02 tonnes, MAC = 0.90

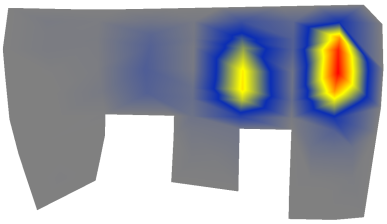

(b) EMA f_1 = 5.24 Hz, ζ = 3.16 %

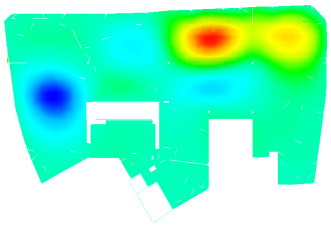

(c) FE analysis, f_2 = 6.52 Hz, m = 28.54 tonnes, MAC = 0.87

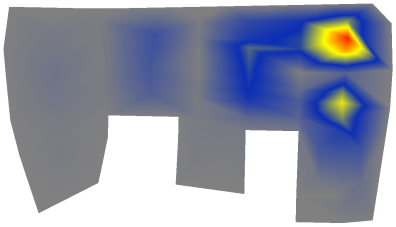

(d) EMA f_2 = 6.06 Hz, ζ = 2.24 %

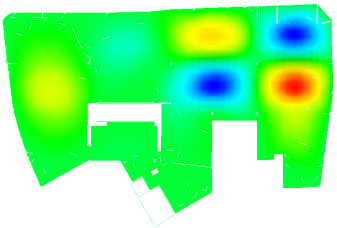

(e) FE analysis, f_3 = 6.33 Hz, m = 35.95 tonnes, MAC = 0.91

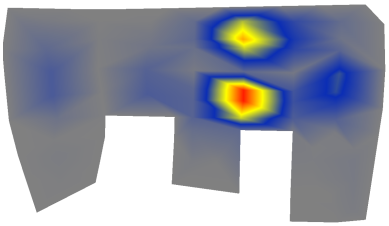

(f) EMA f_3 = 6.58 Hz, ζ = 1.87 %

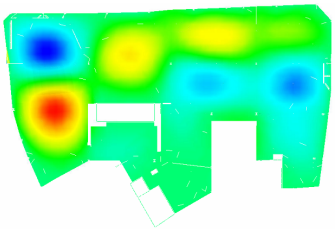

(g) FE analysis, f_4 = 6.87 Hz, m = 39.95 tonnes, MAC = 0.89

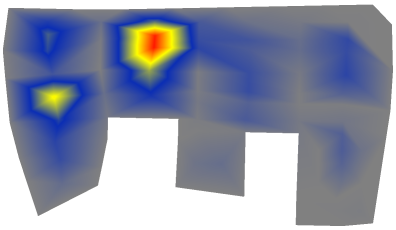

(h) EMA f_4 = 7.31 Hz, ζ = 1.7 %

Fig. 8. FS1 vibration modes from FE Analysis and Experimental Modal Analysis

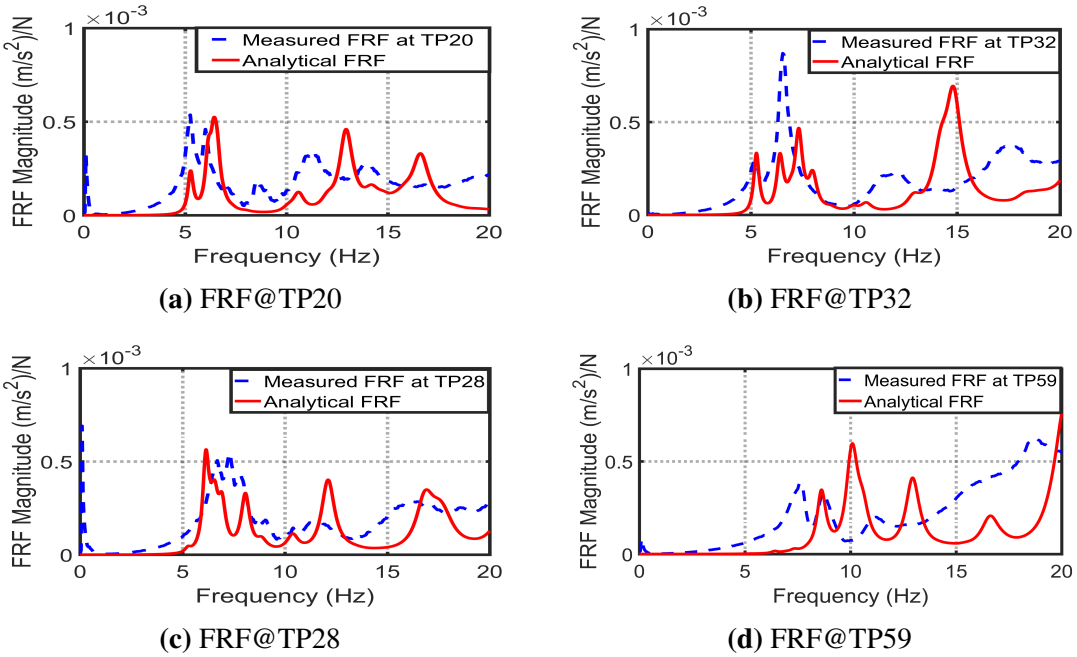

(a) FRF@TP20 **(b)** FRF@TP32

(c) FRF@TP28 **(d)** FRF@TP59

Fig. 9. Comparison of experimental FRFs and those from the updated FE model at four locations on FS1

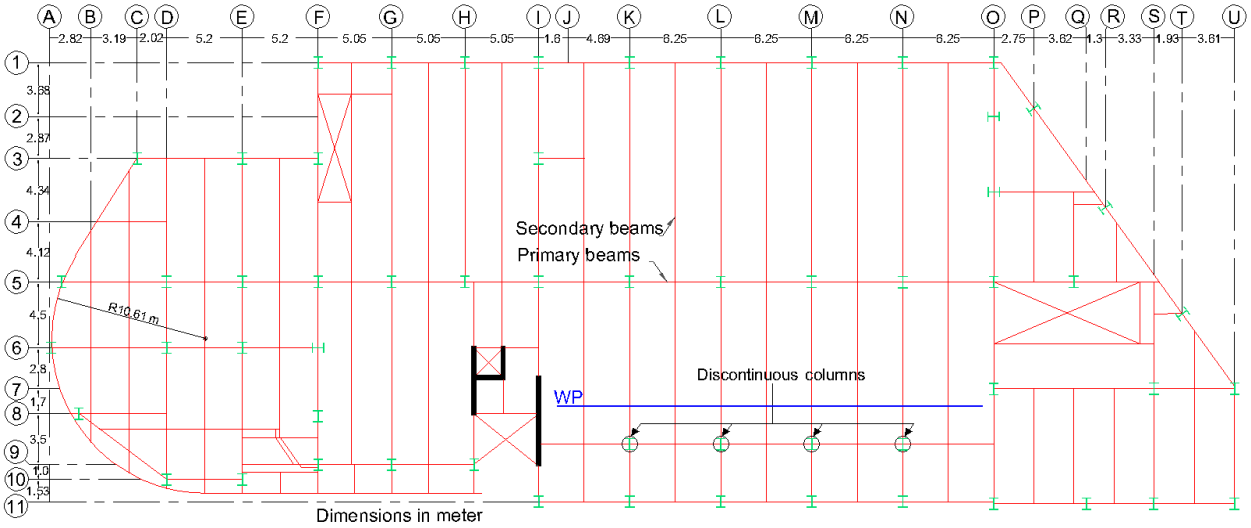

Fig. 10. Plan layout of FS2

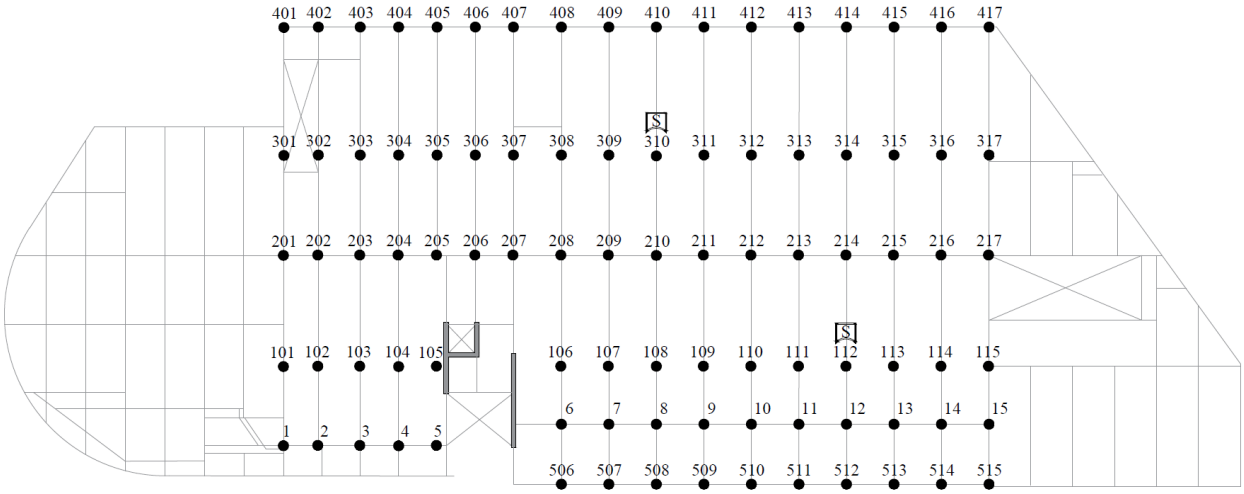

Fig. 11. Test point locations on FS2. Excitation locations are shown by letter “S”.

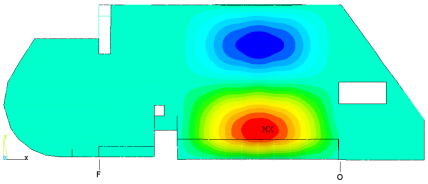

(a) FE analysis, f_1 = 4.88 Hz, m = 85.15 tonnes, MAC = 0.98

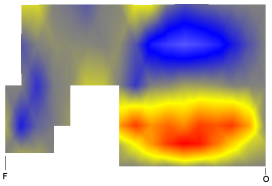

(b) EMA f_1 = 4.92 Hz, ζ = 0.66 %

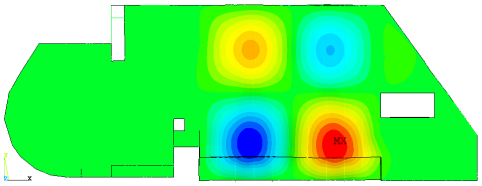

(c) FE analysis, f_2 = 5.43 Hz, m = 92.89 tonnes, MAC = 0.94

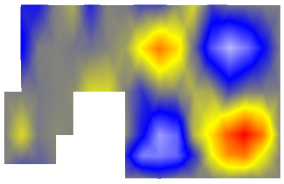

(d) EMA f_2 = 5.51 Hz, ζ = 0.74 %

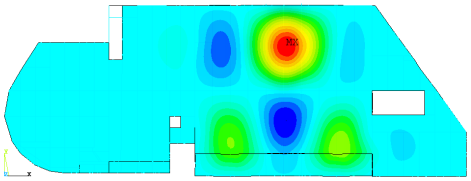

(e) FE analysis, f_3 = 6.41 Hz, m = 32.02 tonnes, MAC = 0.93

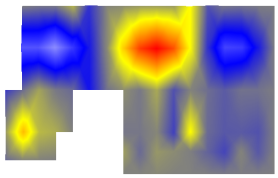

(f) EMA f_3 = 6.12 Hz, ζ = 0.32 %

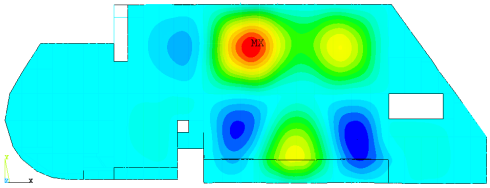

(g) FE analysis, f_4 = 6.48 Hz, m = 33 tonnes, MAC = 0.91

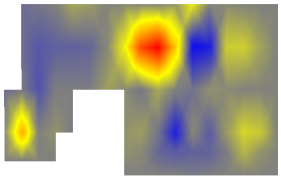

(h) EMA f_4 = 6.55 Hz, ζ = 0.32 %

Fig. 12. FS2 vibration modes from FE Analysis and Experimental Modal Analysis

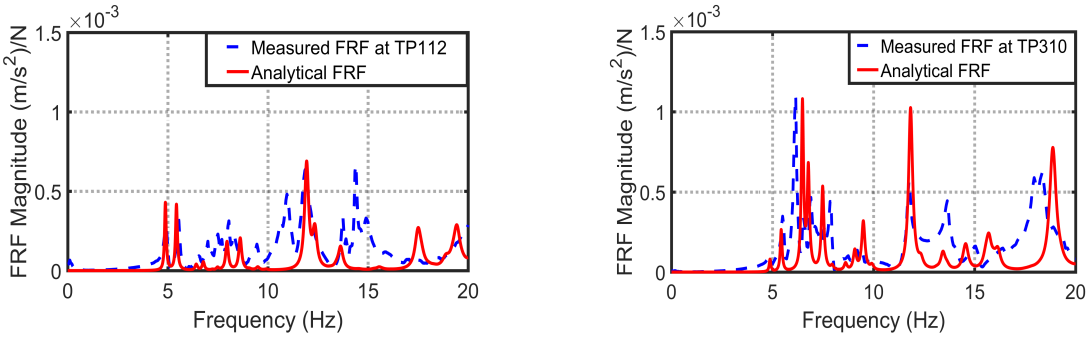

(a) FRF@TP112 **(b)** FRF@TP310

Fig. 13. Comparison of experimental FRFs and those from the updated FE model at two locations on FS2

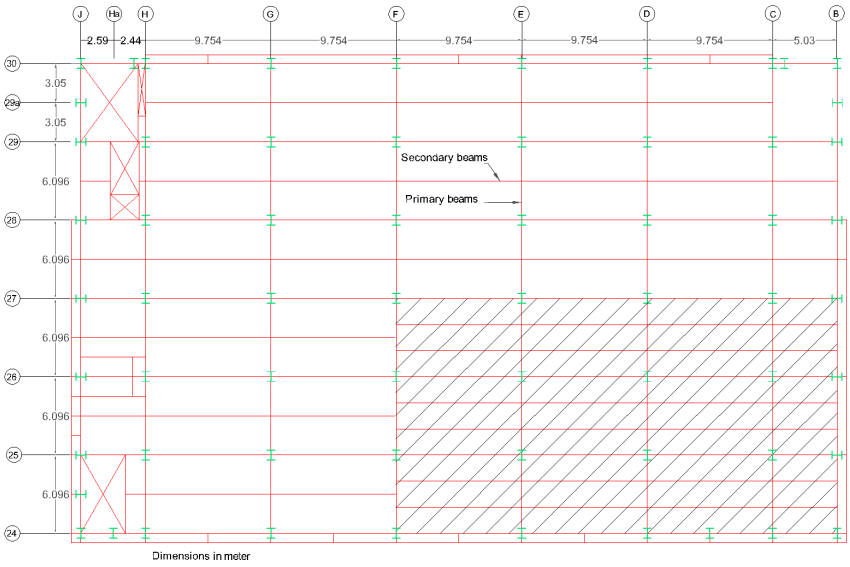

Fig. 14. Plan layout of FS3

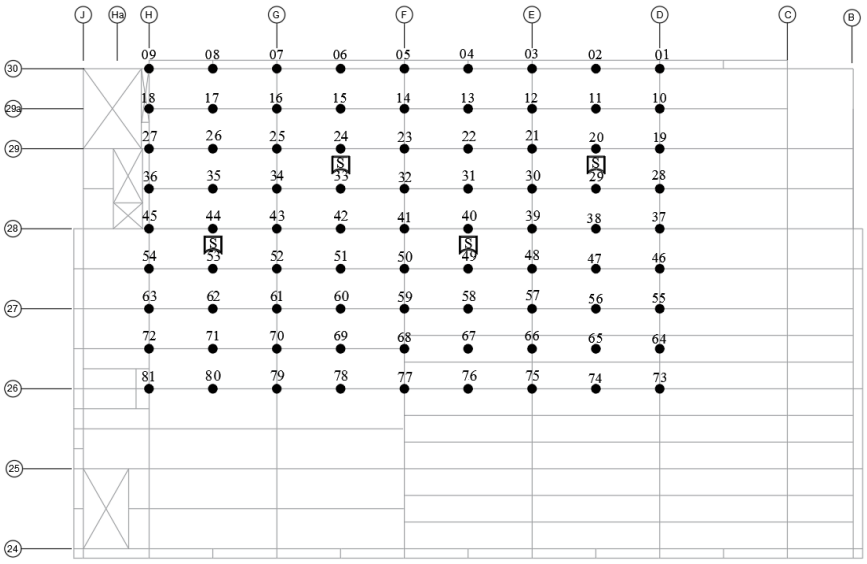

Fig. 15. Test point locations on FS3. Excitation locations are shown by the letter "S".

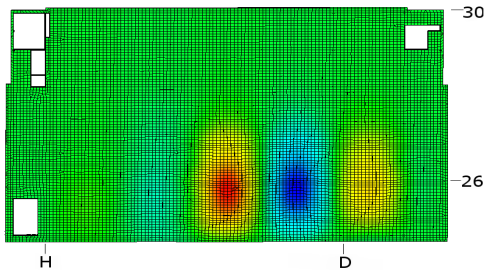

(a) FE analysis, f_1 = 6.57 Hz, m = 114.6 tonnes, MAC = 0.88

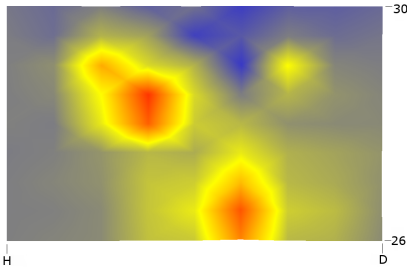

(b) EMA f_1 = 6.56 Hz, ζ = 1.0 %

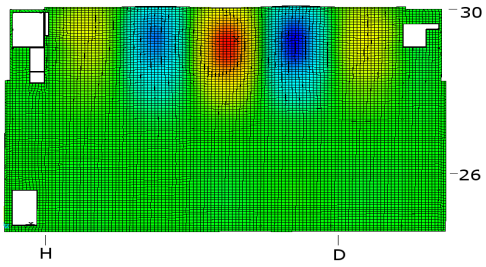

(c) FE analysis, f_2 = 6.84 Hz, m = 96.15 tonnes,, MAC = 0.85

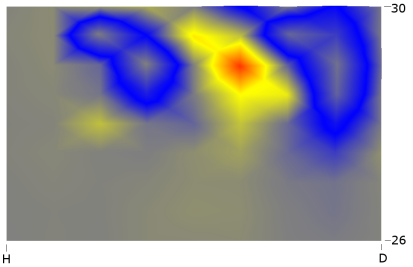

(d) EMA f_2 = 6.89 Hz, ζ = 1.04 %

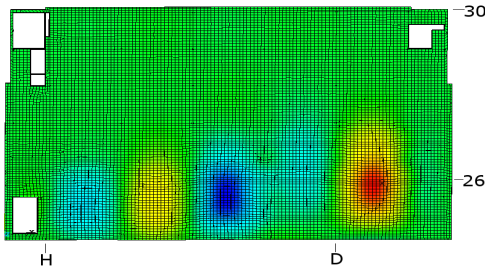

(e) FE analysis, f_3 = 7.23 Hz, m = 104.13 tonnes

Mode not measured

(f) EMA f_3 = 0, ζ = 0 %

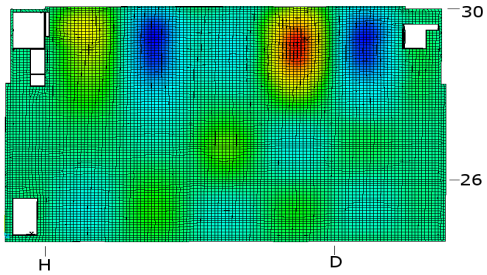

(g) FE analysis, f_4 = 7.4 Hz, m = 104.53 tonnes, MAC = 0.87

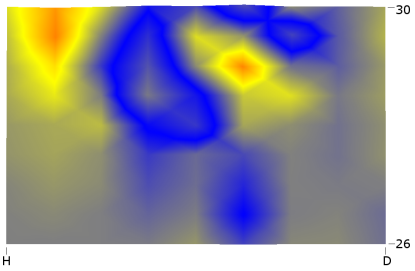

(h) EMA f_4 = 7.39 Hz, ζ = 0.62 %

Fig. 16. FS3 vibration modes from FE Analysis and Experimental Modal Analysis

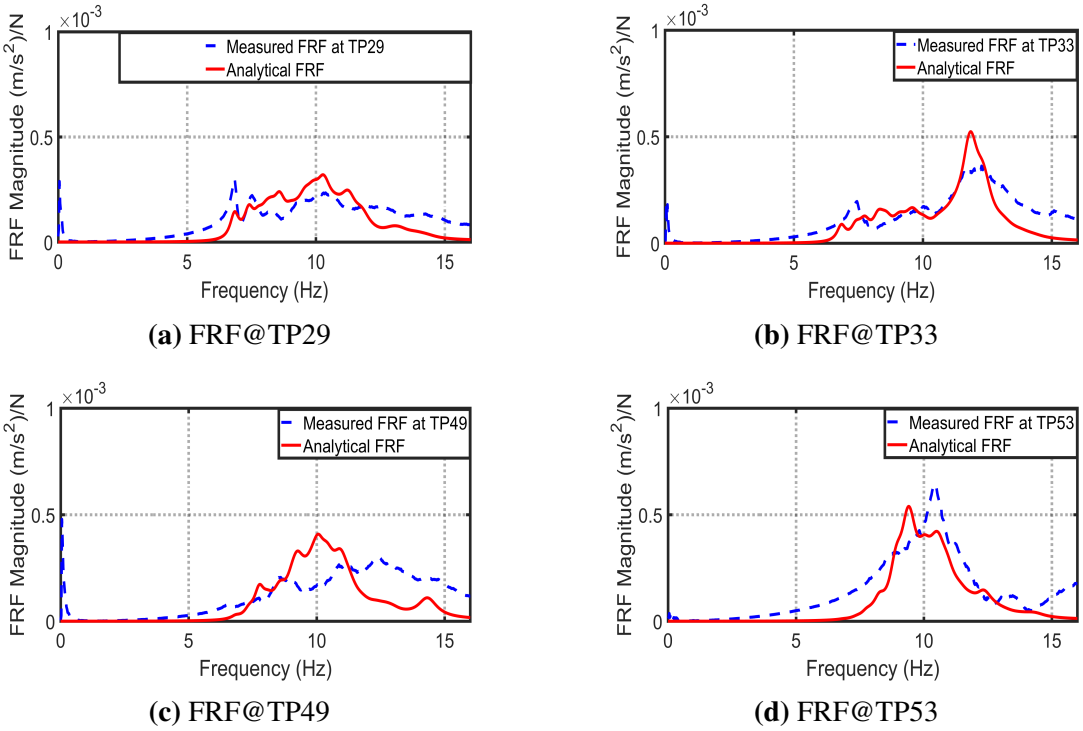

(a) FRF@TP29 **(b)** FRF@TP33

(c) FRF@TP49 **(d)** FRF@TP53

Fig. 17. Comparison of experimental FRFs and those from the updated FE model at four locations on FS3

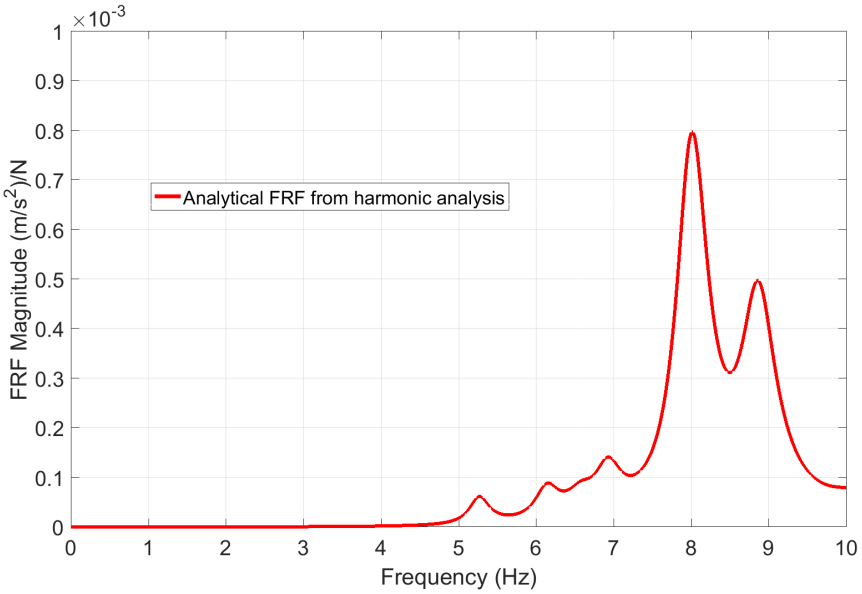

Fig. 18. Peak FRF magnitude from FE harmonic analysis between grid line B-1 & C-2

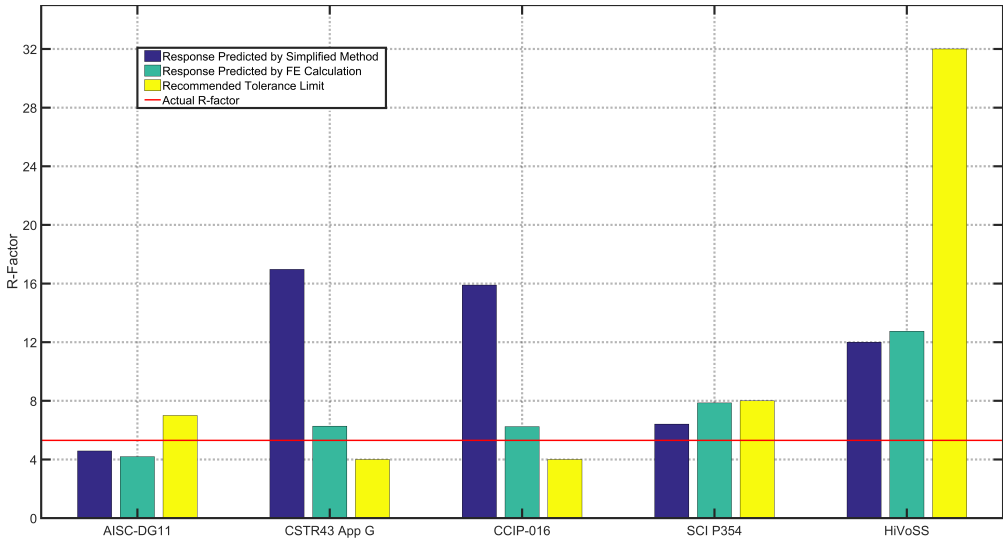

Fig. 19. FS1 Response prediction of guidelines against actual measured response

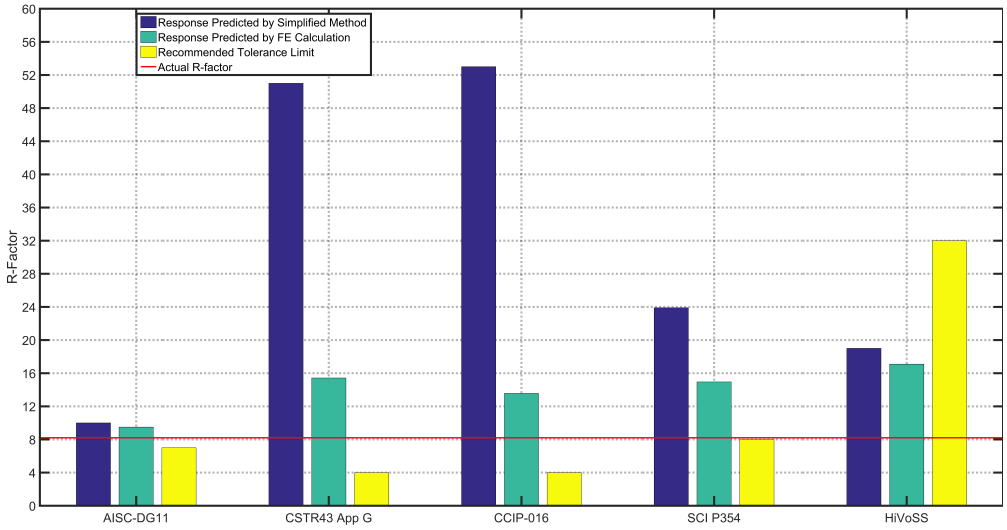

Fig. 20. FS2 Response prediction of guidelines against actual response

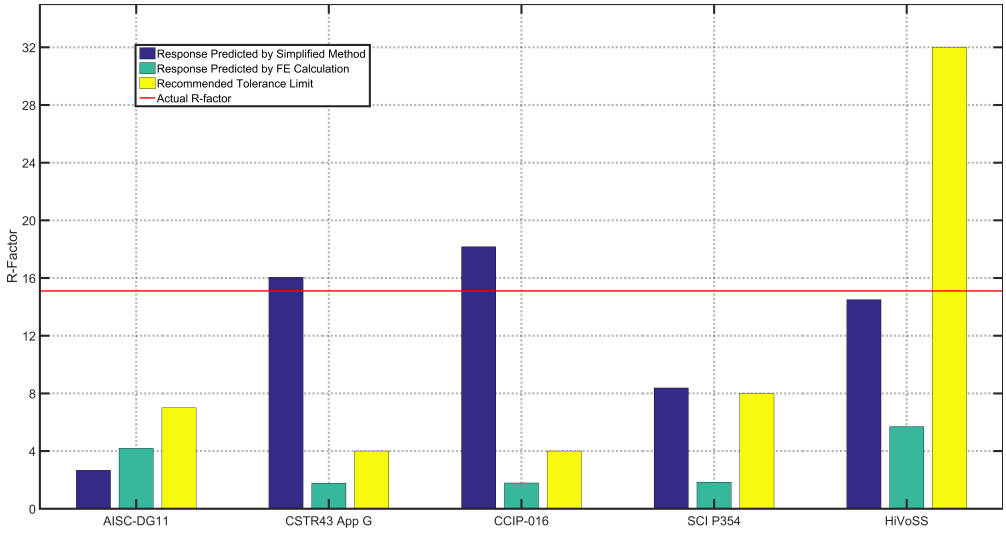

Fig. 21. FS3 Response prediction of guidelines against actual response